Effects of Site-Directed Mutations on Heme Reduction in *Escherichia coli* Nitrate Reductase A by Menaquinol: A Stopped-Flow Study†

Zhongwei Zhao, Richard A. Rothery, and Joel H. Weiner*

CIHR Membrane Protein Research Group, Department of Biochemistry, 474 Medical Sciences Building, University of Alberta, Edmonton, Alberta T6G 2H7, Canada

Received June 23, 2003; Revised Manuscript Received September 22, 2003

ABSTRACT: We have studied the effects of site-directed mutations in *Escherichia coli* nitrate reductase A (NarGHI) on heme reduction by a menaquinol analogue (menadiol) using the stopped-flow method. For NarGHI^{H66Y} and NarGHI^{H187Y}, both lacking heme b_L but having heme b_H, the heme reduction by menadiol is abolished. For NarGHI^{H56R} and NarGHI^{H205Y}, both without heme b_H but with heme b_L, a smaller and slower heme reduction compared to that of the wild-type enzyme is observed. These results indicate that electrons from menadiol oxidation are transferred initially to heme b_L. A transient species, likely to be associated with a semiquinone radical anion, was generated not only on reduction of the wild-type enzyme as observed previously (*1*) but also on reduction of NarGHI^{H56R} and NarGHI^{H205Y}. The inhibitors 2-*n*-heptyl-4-hydroxyquinoline-*N*-oxide and stigmatellin both have significant effects on the reduction kinetics of NarGHI^{H56R} and NarGHI^{H205Y}. We have also investigated the reoxidation of menadiol-reduced heme by nitrate in the mutants. Compared to the wild type, no significant heme reoxidation is observed for NarGHI^{H56R} and NarGHI^{H205Y}. This result indicates that a single mutation removing heme b_H blocks the electron-transfer pathway from the subunit NarI to the catalytic dimer NarGH.

Escherichia coli can grow anaerobically by developing specialized respiratory chains that consist of a group of primary dehydrogenases, an intermediate electron carrier (menaquinol, MQH_2;[1] ubiquinol, UQH_2; or demethylmenaquinol, $DMQH_2$), and a series of terminal reductases (*2*). Nitrate reductase A (NarGHI), a heme containing iron−sulfur molybdoenzyme, is one of these terminal reductases. It consists of a catalytic subunit (NarG, 140 kDa) having a molybdobis(molybdopterin guanine dinucleotide) cofactor (Mo-bisMGD) at its active site (*3*, *4*), an electron-transfer subunit (NarH, 58 kDa) with four iron−sulfur clusters (three [4Fe−4S] clusters and one [3Fe−4S] cluster) (*3*, *5*, *6*), and a membrane anchor subunit (NarI, 26 kDa) with two hemes (one, heme b_H, has a higher midpoint potential E_m of +120 mV, and the other, heme b_L, a lower midpoint potential E_m of +20 mV) (*7*−*9*). The NarG and NarH subunits are anchored by the NarI subunit to the inner surface of the cytoplasmic membrane as an NarGH catalytic dimer.

NarGHI catalyzes MQH_2 or UQH_2 oxidation, accompanied by release of protons at the periplasmic side of the membrane, and nitrate reduction by consumption of protons at the cytoplasmic side of the membrane (*10*−*13*). On the basis of available data from biochemical and biophysical studies (for reviews, see refs *12*, *14*, and *15*), it has been proposed that electrons from quinol oxidation are transferred from an MQH_2/UQH_2 binding site (Q-site) located toward the periplasmic side of the NarI subunit (*16*), via hemes b_L and b_H, the [3Fe−4S] cluster, and some or all of the remaining [4Fe−4S] clusters located in the NarH subunit, to the Mo-bisMGD cofactor of the NarG subunit (*3*, *8*).

A number of steady-state kinetic studies (*17*, *18*) and spectrophotometric studies (*16*, *19*) have been carried out on the interaction of quinol with *E. coli* nitrate reductase. It was observed in the conventional spectrophotometric studies that the reduction of the hemes in NarGHI by MQH_2 takes several seconds to complete (*16*, *19*). However, due to the limitations of the spectrophotometric techniques employed, it was not possible to investigate the initial fast reaction processes occurring during the first few seconds in detail. Recently, the first transient kinetic study on heme reduction in NarGHI was reported by us (*1*). Using the stopped-flow technique, we were able to study the initial fast reactions that occur immediately after mixing NarGHI with menaquinol on the previously uncharacterized time scale. We found that the heme reduction in NarGHI by menadiol exhibits four phases. A transient species, described as a complex of menaquinone radical anion ($MQ^{\bullet -}$) associated with the enzyme, is kinetically correlated to the reduction of the hemes (*1*).

On the basis of site-directed mutagenesis studies, it has been shown that the NarI−H-66 and NarI−H-187 coordinate heme b_L is located close to the periplasmic side of the membrane and the NarI−H-56 and NarI−H-205 coordinate

† This work was funded by grants from the Canadian Institutes of Health Research (CIHR) and the Human Frontier Science Program Organization to J.H.W. J.H.W. is a Canada Research Chair in Membrane Biochemistry.

* To whom correspondence should be addressed. Phone: (780) 492 2761. Fax: (780) 492 0886. E-mail: joel.weiner@ualberta.ca.

[1] Abbreviations: DmsABC, *E. coli* DMSO reductase; EPR, electron paramagnetic resonance; FrdABCD, *E. coli* fumarate reductase; HOQNO, 2-*n*-heptyl-4-hydroxyquinoline-*N*-oxide; Mo-bisMGD, molybdobis(molybdopterin guanine dinucleotide) cofactor; MQ, menaquinone; MQH_2, menaquinol; NarGHI, *E. coli* nitrate reductase A; NarI(ΔGH), nitrate reductase cytochrome *b* subunit in the absence of the NarGH dimer; STIG, stigmatellin; UQH_2, ubiquinol.

10.1021/bi0350856 CCC: $25.00
Published on Web 11/13/2003

heme b_H is close to the cytoplasmic side (*20*). To understand the role of the two hemes in the electron-transfer pathway of NarGHI, several mutants have been constructed and expressed. These include NarGHI^{H66Y} and NarGHI^{H187Y} without heme b_L, NarGHI^{H56R} and NarGHI^{H205Y} lacking heme b_H, and NarI(ΔGH) lacking subunits NarG and NarH. However, a stopped-flow (transient kinetic) study for the effect of mutations in NarI on heme reduction by MQH_2 has not been reported.

The quinol-binding-site inhibitor 2-*n*-heptyl-4-hydroxyquinoline-*N*-oxide (HOQNO) is a structural analogue of MQH_2. It has been shown that both HOQNO and stigmatellin (STIG) can inhibit quinol:nitrate oxidoreductase activity (*16*). The binding of HOQNO to NarGHI causes an inversion of the midpoint potentials (E_m) of the two hemes, whereas the binding of STIG results in a moderate increase of E_m of heme b_L (*9*). Previously, we have applied the stopped-flow technique to investigate the binding of HOQNO with other terminal reductases in respiratory chains of *E. coli*, such as dimethyl sulfoxide reductase (DmsABC) (*21*) and fumarate reductase (FrdABCD) (*22*). More recently, we have studied the inhibitory effect of HOQNO and STIG on heme reduction by menadiol in the wild-type NarGHI using the stopped-flow technique (*1*). HOQNO and STIG have exhibited significant and different inhibitory effects on the heme reduction. For NarGHI^{H66Y}, NarGHI^{H187Y}, NarGHI^{H56R}, and NarGHI^{H205Y}, however, the effect of HOQNO and STIG on the heme reduction has not been investigated using the stopped-flow technique.

Several semiquinone radical species have been detected in mutant or wild-type enzymes of *E. coli* respiratory chains, such as FrdABCD (*23*) and quinol oxidases cytochrome *bd* (*24*) and cytochrome bo_3 (*25*), using electron paramagnetic resonance (EPR) spectroscopy. In the mutants NarGH^{C16A}I and NarGH^{C263A}I, an HOQNO-sensitive semiquinone radical species was observed using EPR (*8*). It is believed that the mutations reduce the rate of the electron transfer in NarGHI, which stabilizes the radical species and makes it possible to be observed. In a previous stopped-flow study, we observed a transient species formed during heme reduction of the wild-type NarGHI, which was likely to be associated with a semiquinone radical anion (*1*). Whether a transient species would be generated during the heme reduction in the mutants, and if so, what effect these mutations would have on the transient species are not known.

In this study, we have utilized the stopped-flow technique to investigate the effects of mutations NarI-H66Y, NarI-H187Y, NarI-H56R, and NarI-H205Y on the heme reduction in NarGHI by a menaquinol analogue (menadiol), and on the heme reoxidation by nitrate. We have also studied the inhibitory effects of the quinol-binding-site inhibitors HOQNO and STIG on the heme reduction in the mutants.

MATERIALS AND METHODS

Bacterial Strains and Plasmids. E. coli LCB2048 [*thi-1, thr-1, leu-6, lacY1, supE44, rpsL175* Δ*nar25*(*narG-narH*) Δ(*nar′U-narZ′*), Ω (Spc^R), Km^R] (*26*) was used for expressing wild-type NarGHI. Wild-type NarGHI and mutants NarI^{H66Y}, NarI^{H187Y}, NarI^{H56R}, and NarI^{H205Y} were expressed from plasmids pVA700, pVA700-H56R, pVA700-H66Y, pVA700-H187Y, and pVA700-H205Y, respectively. Plasmid pCD7 was used to express a mutant NarI(ΔGH) that was not assembled in the presence of the catalytic dimer NarGH (*6*, *8*).

Growth of Cells and Preparation of Membrane Vesicles. LCB2048/pVA700 cells were grown microaerobically in 2 L batches at 30 °C and pH 7.0, and enzyme overexpression was induced with 1 mM isopropyl 1-thio-β-D-galactopyranoside (IPTG) as previously described (*1*). Cells were prepared by passage through a French pressure cell and differential centrifugation as described previously (*27*). LCB2048 membranes lacking NarGHI were prepared by the same method as above except that ampicillin and IPTG were not used in the growth medium. LCB2048/pCD7 cells (overexpressing NarI(ΔGH)) were grown on Terrific Broth, as previously described (*9*). The cytoplasmic membranes were isolated as described above. Protein concentrations were determined by a modified Lowry assay in the presence of 1% SDS using a BioRad serum albumin protein standard (*28*).

NarGHI comprised approximately 57% of total proteins as determined by Coomassie Blue gel densitometry (*9*). Furthermore, it was clear that the concentration of other heme-containing proteins in the membranes was insignificant. The absorption spectrum of dithionite-reduced membranes of *E. coli* (LCB2048) lacking nitrate reductase did not show any heme absorption bands in the wavelength region from 350 to 600 nm, confirming the lack of other heme-containing proteins in the membranes. The absorption spectrum in the visible region for the native nitrate reductase as prepared had a single peak at 415 nm (data not shown). After addition of sodium dithionite to the enzyme sample, the absorption spectrum observed was typical of reduced hemes exhibiting three bands at 560 nm (the α band), 530 nm (the β band), and 430 nm (the γ band) (data not shown), indicating that both hemes in the enzyme were in the oxidized state initially. These spectra were very similar to those published by Morpeth and Boxer (*17*) for the native and the dithionite-reduced nitrate reductase of *E. coli*.

Preparation of Stock Solutions. Menadione (2-methyl-1,4-naphthoquinone) was purchased from Sigma-Aldrich. Stock solutions of menadione were prepared by dissolving it in pure ethanol and stored at −20 °C in the dark. Menadiol was prepared by reducing menadione with zinc in an acidic ethanol solution just before use as described previously (*29*), placed on ice, and protected from light. Potassium nitrate (Sigma-Aldrich) was used to prepare the stock solution of nitrate.

Stopped-Flow Experiments and Data Analysis. Stopped-flow experiments were performed using a Sequential Bio SX-17MV stopped-flow spectrofluorimeter (Applied Photophysics Ltd., Leatherhead, U.K.) with a 1 cm path length at 25 °C. The flow system was flushed thoroughly with N_2-saturated buffer (100 mM MOPS and 5 mM EDTA, pH 7.0) before the experiments. All solutions were saturated with N_2, kept under a N_2 atmosphere, and protected from light during the experiments. Unless otherwise stated, all concentrations quoted were the initial concentrations before mixing, and the mixing ratios of two solutions were all 1:1. Since the reduced forms of the hemes in NarGHI have higher absorption at 560 nm compared to the oxidized forms (*16*), the reduction (causing the absorbance to increase) and the oxidation (causing the absorbance to decrease) of the hemes

can be followed spectrophotometrically. In a typical experiment, 1 mg mL^{-1} NarGHI or mutant (estimated to be 2 μM, on the basis of EPR spin quantitation (*9*)) in 100 mM MOPS and 5 mM EDTA (pH 7.0) in the absence or in the presence of the inhibitors was rapidly mixed with an equal volume of 500 μM menadiol in the same buffer. We found that heme reduction kinetics was relatively independent of menadiol concentration in the range from 350 to 650 μM (before the mixing). Therefore, 500 μM menadiol was chosen for all experiments. For the inhibitors HOQNO and STIG, it was shown that maximum inhibition can be achieved at the inhibitor concentration of 60 μM (*16*). Thus, 60 μM HOQNO or STIG was used to incubate with the enzyme for all inhibition studies.

To investigate the reoxidation of the menadiol-reduced hemes in NarGHI by nitrate, a sequential mixing method was utilized. In this method, 1 mg mL^{-1} NarGHI or mutant in 100 mM MOPS and 5 mM EDTA (pH 7.0) was first rapidly mixed with an equal volume of 500 μM menadiol in the same buffer. After being aged for 50 s to allow the complete reduction of the hemes, this mixture was then rapidly mixed with an equal volume of 1 mM nitrate, and the reoxidation process was followed at 560 nm.

In both single and sequential mixing experiments, at least three runs were performed for each time scale and 2000 data points were collected at both wavelengths of 560 and 575 nm (as reference). The raw data were averaged, and the data for the reduction or reoxidation of the hemes were obtained by subtracting the reference data collected at 575 nm from the data obtained at 560 nm. The background absorbance from LCB2048 membranes lacking NarGHI was also subtracted from these data. After subtraction, the data were fitted to an appropriate equation using the software supplied by Applied Photophysics. The absorbance changes observed for the reduction of hemes by menadiol (ΔAbs) were fitted to a double-exponential equation:

$$\Delta\text{Abs} = A_1 e^{-k_1 t} + A_2 e^{-k_2 t} + b \qquad (1)$$

where A_1, A_2, and A are the amplitudes and k_1, k_2, and k the rate constants and t is time and b the end point of the data trace.

A transient species was formed during heme reduction by menadiol in NarGHI, NarGHI^{H56R}, NarGHI^{H205Y}, and NarI-(ΔGH). It was observed at 390 nm, where the semiquinone radical anion of menadione has its maximum absorption (*30*, *31*).

RESULTS

Effects of NarI-H56R, NarI-H205Y, NarI-H66Y, and NarI-H187Y Mutations on Heme Reduction by Menadiol. These mutations affected the heme reduction significantly as shown in Figure 1. The absorbance traces observed at 560 nm in Figure 1 were obtained by rapidly mixing 1 mg mL^{-1} wild-type-NarGHI- or the mutant-containing membranes (2 μM; see the Materials and Methods) with 500 μM menadiol in 100 mM MOPS and 5 mM EDTA (pH 7.0) at 25 °C. The background absorbance obtained by mixing 1 mg mL^{-1} LCB2048 membranes lacking NarGHI with the menadiol solution was subtracted from each of these traces, and the common reference point of the absorbance was obtained. After the membranes containing enriched wild-type NarGHI were rapidly mixed with the menadiol solution (trace 1), an increase of the absorbance at 560 nm (after the absorbance at 575 nm was subtracted) was observed, indicating that the reduction of the hemes occurred. Furthermore, the change of the absorbance exhibited four phases; a very fast increase in the absorbance (phase 1), a slower decrease lasting for about 1 s (phase 2), a relatively fast increase (phase 3), and a slow increase (phase 4) were observed sequentially with time (the data for the wild-type enzyme have been published recently (*1*) and are shown here for comparison with the data from the mutants).

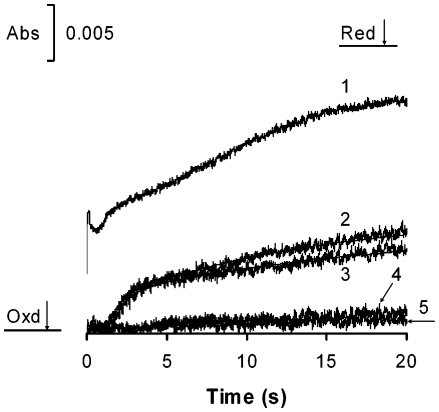

FIGURE 1: Effects of NarI-H56R, NarI-H205Y, NarI-H66Y, and NarI-H187Y mutations on heme reduction by menadiol observed at 560 nm on a 20 s time scale. The absorbance traces were observed after rapid mixing of 1 mg mL^{-1} wild-type NarGHI (trace 1) and mutants NarGHI^{H56R} (trace 2), NarGHI^{H205Y} (trace 3), NarGHI^{H66Y} (trace 4), and NarGHI^{H187Y} (trace 5) with 500 μM menadiol in 100 mM MOPS and 5 mM EDTA (pH 7.0) at 25 °C. The smooth solid lines in traces 2 and 3 show the kinetic fits to eq 1, which gives the rate constants $k_1 = 1.60 \pm 0.2$ s^{-1} and $k_2 = 0.076 \pm 0.008$ s^{-1}, the amplitudes $A_1 = -0.0024$ and $A_2 = -0.0068$, and the residual of the fit of less than ± 0.00087 (not shown) for NarGHI^{H56R} (trace 2), and the rate constants $k_1 = 1.27 \pm 0.13$ s^{-1} and $k_2 = 0.053 \pm 0.005$ s^{-1}, the amplitudes $A_1 = -0.0043$ and $A_2 = -0.0056$, and the residual of the fit of less than ± 0.001 (not shown) for NarGHI^{H205Y}. The absorbance levels of the fully oxidized and reduced enzymes are indicated by the arrows labeled as "oxd" and "red", respectively.

A detailed description of these kinetic phases was proposed in our recent publication (*1*). The fast reduction of heme b_L (phase 1) resulted from the transfer of the first electron from the menadiol, bound to the enzyme, after mixing. The electron was next transferred from the reduced heme b_L to oxidized heme b_H. The reduced heme b_H in turn transferred the electron to the iron−sulfur clusters, resulting in heme reoxidation observed as phase 2. Phase 3 was attributed to the second reduction of hemes resulting from the transfer of a second electron from a semimanaquinone radical anion, formed by menadiol losing one electron and two protons. Phase 4 was assigned to the subsequent overall heme reduction induced by receipt of electrons from the second, third, or more menadiol molecules, depending on how many iron−sulfur clusters were reduced in addition to the reduction of Mo(VI) to Mo(IV) and the reduction of two hemes. Since 2000 data points were acquired on a 20 s time scale, at the first data point (0.01 s after mixing) a significant portion of the reduction had already occurred. The total reduction was calculated using the final value of the reduction trace observed at 560 nm 100 s after mixing (see below). Both phase 1 and phase 3 were fitted to the double-exponential

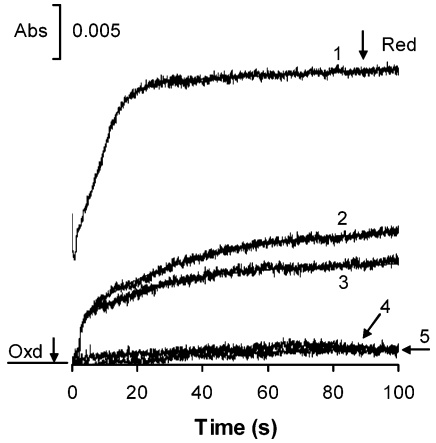

FIGURE 2: Effects of NarI-H56R, NarI-H205Y, NarI-H66Y, and NarI-H187Y mutations on heme reduction by menadiol observed at 560 nm on a 100 s time scale. The absorbance traces were observed after rapid mixing of 1 mg mL^{-1} wild-type NarGHI (trace 1) and mutants NarGHI^{H56R} (trace 2), NarGHI^{H205Y} (trace 3), NarGHI^{H66Y} (trace 4), and NarGHI^{H187Y} (trace 5) with 500 μM menadiol in 100 mM MOPS and 5 mM EDTA (pH 7.0) at 25 °C. The smooth solid lines in traces 2 and 3 show the kinetic fits to eq 1, giving the rate constants $k_1 = 0.78 \pm 0.08$ s^{-1} and $k_2 = 0.03 \pm 0.003$ s^{-1}, the amplitudes $A_1 = -0.0019$ and $A_2 = -0.0064$, and the residual of the fit of less than ± 0.00083 (not shown) for NarGHI^{H56R} (trace 2), and the rate constants $k_1 = 0.04 \pm 0.004$ s^{-1} and $k_2 = 0.002 \pm 0.0002$ s^{-1}, the amplitudes $A_1 = -0.0038$ and $A_2 = -0.0025$, and the residual of the fit of less than ± 0.0007 (not shown) for NarGHI^{H205Y}. The absorbance levels of the fully oxidized and reduced enzymes are indicated by the arrows labeled as "oxd" and "red", respectively.

equation (eq 1) that gave the rate constants k_1 and k_2 of 412 $\pm$ 40 and 73 $\pm$ 7 s^{-1} for phase 1 and 9.24 $\pm$ 0.9 and 0.22 $\pm$ 0.02 s^{-1} for phase 3 (*1*).

Mutations of the heme-binding residues had significant effects on the heme reduction by menadiol as shown in Figure 1. For NarGHI^{H56R} (trace 2) and NarGHI^{H205Y} (trace 3), without heme b_H but having heme b_L, after a lag phase lasting about 2 s, a relatively fast reduction phase followed by a slow reduction phase was observed. These traces were fitted to the double-exponential equation (eq 1), which gave the rate constants k_1 of 1.60 $\pm$ 0.2 s^{-1} and k_2 of 0.076 $\pm$ 0.008 s^{-1} for NarGHI^{H56R}, and k_1 of 1.27 $\pm$ 0.13 s^{-1} and k_2 of 0.053 $\pm$ 0.005 s^{-1} for NarGHI^{H205Y}. Compared to the wild-type enzyme (trace 1), the heme reduction in NarGHI^{H56R} (trace 2) and NarGHI^{H205Y} (trace 3) showed two distinct features. First, there was a lag phase for the heme reduction in both mutants. Second, there was no heme reoxidation corresponding to phase 2 observed for the wild-type enzyme. For the mutants NarGHI^{H66Y} (trace 4) and NarGHI^{H187Y} (trace 5), lacking heme b_L and having heme b_H, heme reduction was totally abolished, indicating that in the absence of heme b_L menadiol was not able to deliver electrons to heme b_H.

To examine the kinetic feature of the heme reduction on a longer time scale, the same experiments as shown in Figure 1 were repeated on a 100 s time scale (Figure 2). For the wild-type enzyme, after NarGHI-enriched membranes were rapidly mixed with the menadiol solution (trace 1), the four phases of heme reduction as described in Figure 1 were observed. On this time scale, different effects of the mutations on the heme reduction were much more clearly observed than on a 20 s time scale. For NarGHI^{H56R} (trace 2) and NarGHI^{H205Y} (trace 3), without heme b_H but having heme b_L, after the lag phase a relatively fast reduction phase followed by a slow reduction phase was observed. These traces were fitted to eq 1, giving the rate constants k_1 of 0.78 $\pm$ 0.08 s^{-1} and k_2 of 0.03 $\pm$ 0.003 s^{-1} for NarGHI^{H56R}, and k_1 of 0.04 $\pm$ 0.004 s^{-1} and k_2 of 0.002 $\pm$ 0.0002 s^{-1} for NarGHI^{H205Y}. The magnitude of heme reduction in NarGHI^{H56R} (trace 2) was bigger than that in NarGHI^{H205Y} (trace 3). For NarGHI^{H66Y} (trace 4) and NarGHI^{H187Y} (trace 5), lacking heme b_L but with heme b_H, no reduction was detected even on this extended time scale. As shown in Figures 1 and 2, heme b_H alone could not be reduced by menaquinol in the absence of heme b_L. Kinetic constants of heme reduction by menadiol in NarGHI, NarGHI^{H56R}, NarGHI^{H205Y}, NarGHI^{H66Y}, and NarGHI^{H187Y} are summarized in Table 1.

Table 1: Observations and Kinetic Constants of Heme Reduction Obtained after Mixing of 1 mg mL^{-1} NarGHI, NarGHI^{H56R}, NarGHI^{H205Y}, NarGHI^{H66Y}, or NarGHI^{H187Y} with 500 μM Menadiol in 100 mM MOPS and 5 mM EDTA (pH 7.0) at 25 °C

		heme reduction		
sample	time scale (s)	k_1 (s^{-1})	k_2 (s^{-1})	ref
NarGHI	0.1, phase 1	412 $\pm$ 40	73 $\pm$ 7.0	1
NarGHI	5, phase 3	9.24 $\pm$ 0.9	0.22 $\pm$ 0.02	1
NarGHI^{H56R}	20	1.60 $\pm$ 0.2	0.076 $\pm$ 0.008	this work
NarGHI^{H56R}	100	0.78 $\pm$ 0.08	0.03 $\pm$ 0.003	this work
NarGHI^{H205Y}	20	1.27 $\pm$ 0.13	0.053 $\pm$ 0.005	this work
NarGHI^{H205Y}	100	0.04 $\pm$ 0.004	0.002 $\pm$ 0.0002	this work
NarGHI^{H66Y}	20 and 100	not observed		this work
NarGHI^{H187Y}	20 and 100	not observed		this work

Inhibitory Effects of HOQNO and STIG on Heme Reductions in NarGHI^{H56R} and NarGHI^{H205Y}. To investigate the effect of HOQO and STIG on heme reduction in NarGHI^{H56R}, 1 mg mL^{-1} NarGHI^{H56R}-containing membranes were preincubated with 60 μM HOQNO or STIG, respectively, and then rapidly mixed with 500 μM menadiol in 100 mM MOPS and 5 mM EDTA (pH 7.0) at 25 °C using the stopped-flow technique (Figure 3). Both inhibitors had significant inhibitory effects on heme reduction. The relatively fast heme reduction observed in the absence of the inhibitors (trace 1) disappeared, and a much slower heme reduction lasting over 100 s after the mixing was observed, indicating that binding of HOQNO (trace 2) or STIG (trace 3) slowed electron transfer from quinol/semiquinone species to heme b_L. In the presence of the inhibitors, the double-exponential fits of traces to eq 1 gave rate constants k_1 of 0.28 $\pm$ 0.03 s^{-1} and k_2 of 0.016 $\pm$ 0.002 s^{-1} for HOQNO, and k_1 of 0.19 $\pm$ 0.02 s^{-1} and k_2 of 0.034 $\pm$ 0.003 s^{-1} for STIG.

The effects of HOQNO and STIG on heme reduction in NarGHI^{H205Y} were investigated by preincubating 1 mg mL^{-1} NarGHI^{H205Y}-containing membranes with 60 μM HOQNO or STIG, respectively, and then rapidly mixing them with 500 μM menadiol in 100 mM MOPS and 5 mM EDTA (pH 7.0) at 25 °C using the stopped-flow technique (Figure 4). Both inhibitors also had significant inhibitory effects on heme reduction in this mutant. The relatively fast heme reduction observed in the absence of the inhibitors (trace 1) was replaced by a much slower heme reduction lasting over 100 s after the mixing. In the presence of the inhibitors, the fits of traces 2 and 3 to eq 1 gave rate constants k_1 of 0.034 $\pm$ 0.003 s^{-1} and k_2 of 0.014 $\pm$ 0.001 s^{-1} for HOQNO, and k_1 of 0.035 $\pm$ 0.004 s^{-1} and k_2 of 0.004 $\pm$ 0.0004 s^{-1} for STIG.

Furthermore, these quinol-binding-site inhibitors appeared to exhibit different effects with different mutants. For

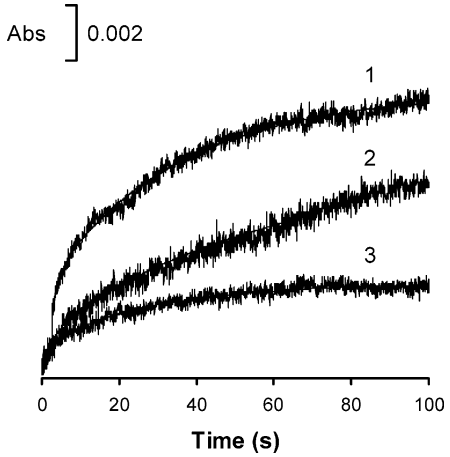

FIGURE 3: Inhibitory effects of HOQNO and STIG on the heme reduction in NarGHI^{H56R}. The absorbance traces were observed at 560 nm after rapid mixing of 1 mg mL^{-1} NarGHI^{H56R} in the absence (trace 1) and in the presence of 60 μM HOQNO (trace 2) or STIG (trace 3) with 500 μM menadiol in 100 mM MOPS and 5 mM EDTA (pH 7.0) at 25 °C. The smooth solid lines in traces 1−3 show the kinetic fits to eq 1, giving the rate constants $k_1 = 0.78 \pm 0.8$ s^{-1} and $k_2 = 0.03 \pm 0.003$ s^{-1}, the amplitudes $A_1 = -0.0019$ and $A_2 = -0.0064$, and the residual of the fit of less than $\pm$ 0.00083 (not shown) for NarGHI^{H56R} (trace 1), the rate constants $k_1 = 0.28 \pm 0.03$ s^{-1} and $k_2 = 0.016 \pm 0.002$ s^{-1}, the amplitudes $A_1 = -0.0011$ and $A_2 = -0.0059$, and the residual of the fit of less than $\pm$0.00089 (not shown) in the presence of HOQNO (trace 2), and the rate constants $k_1 = 0.19 \pm 0.02$ s^{-1} and $k_2 = 0.034 \pm 0.003$ s^{-1}, the amplitudes $A_1 = -0.0006$ and $A_2 = -0.002$, and the residual of the fit of less than $\pm$0.00054 (not shown) in the presence of STIG (trace 3).

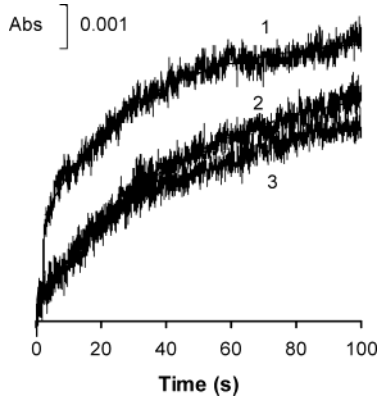

FIGURE 4: Inhibitory effects of HOQNO and STIG on the heme reduction in NarGHI^{H205Y}. The absorbance traces were observed at 560 nm after rapid mixing of 1 mg mL^{-1} NarGHI^{H56R} in the absence (trace 1) and in the presence of 60 μM HOQNO (trace 2) or STIG (trace 3) with 500 μM menadiol in 100 mM MOPS and 5 mM EDTA (pH 7.0) at 25 °C. The smooth solid lines in traces 1−3 show the kinetic fits to eq 1, which gives the rate constants $k_1 = 0.04 \pm 0.004$ s^{-1} and $k_2 = 0.002 \pm 0.0002$ s^{-1}, the amplitudes $A_1 = -0.0038$ and $A_2 = -0.0025$, and the residual of the fit of less than $\pm$0.0007 (not shown) for NarGHI^{H205Y}, the rate constants $k_1 = 0.034 \pm 0.003$ s^{-1} and $k_2 = 0.014 \pm 0.001$ s^{-1}, the amplitudes $A_1 = -0.0026$ and $A_2 = -0.003$, and the residual of the fit of less than $\pm$0.00078 (not shown) in the presence of HOQNO, and the rate constants $k_1 = 0.035 \pm 0.004$ s^{-1} and $k_2 = 0.004 \pm 0.0004$ s^{-1}, the amplitudes $A_1 = -0.0021$ and $A_2 = -0.0014$, and the residual of the fit of less than $\pm$0.00076 (not shown) in the presence of STIG.

NarGHI^{H56R} (Figure 3) the magnitude of the relatively fast reduction phase was reduced significantly in the presence of HOQNO or STIG. However, STIG (trace 3) exhibited a stronger inhibitory effect than HONQO (trace 2) on the slow reduction phase. For NarGHI^{H205Y} (Figure 4), on the other hand, both HOQNO (trace 2) and STIG (trace 3) exhibited a significant inhibitory effect on the relatively fast reduction phase but not on the slow reduction phase. Kinetic constants of heme reduction by menadiol in NarGHI^{H56R} and NarGHI^{H205Y}, obtained in the absence and presence of HOQNO or STIG, are summarized in Table 2.

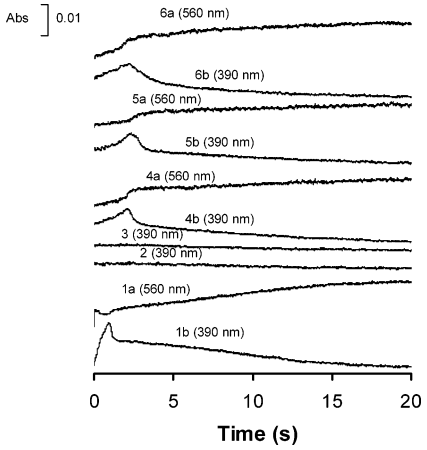

FIGURE 5: Observation of a transient species generated during the heme reduction by menadiol on a 20 s time scale. The absorbance traces were observed after rapid mixing 1 mg mL^{-1} wild-type NarGHI and the mutants with 500 μM menadiol in 100 mM MOPS and 5 mM EDTA (pH 7.0) at 25 °C. Heme reductions were followed at 560 nm, and the corresponding traces were labeled with "a". The formations and decays of the transient species were monitored at 390 nm, and the traces were labeled with "b". Key: traces 1a and 1b, absorbance traces of heme reduction and the transient species, respectively, for the wild-type NarGHI; traces 2 and 3, absorbance traces observed at 390 nm for NarGHI^{H66Y} and NarGHI^{H187Y}, respectively; traces 4a and 4b, for NarGHI^{H56R}; traces 5a and 5b, for NarGHI^{H205Y}; traces 6a and 6b, for NarI(ΔGH). These traces were not shown with a common reference point of absorbance to avoid overlaps of them.

Observation of a Transient Species Generated during Heme Reduction by Menadiol in NarGHI^{H56R} and NarGHI^{H205Y}. It has been reported previously that a mutation in NarGHI stabilized a semiquinone radical species by reducing the rate of electron transfer in NarGHI, which resulted in the observation of the radical species using EPR (*8*). The menadione radical anion has an absorption maximum at 390 nm (*30*, *31*). In this study, therefore, we utilized the stopped-flow technique to detect the formation of the radical species spectrophotometrically. The absorbance traces in Figure 5 were obtained by rapidly mixing 1 mg mL^{-1} wild-type NarGHI and the mutants with 500 μM menadiol in 100 mM MOPS and 5 mM EDTA (pH 7.0) at 25 °C. The heme reduction was followed at 560 nm (575 nm as a reference), and the formation and the decay of the transient species were monitored at 390 nm. For the wild-type enzyme, after being rapidly mixed with the menadiol solution, heme reduction (as described for Figure 1) was observed at 560 nm (trace 1a). The formation and the decay of a transient species were observed at 390 nm on the same time scale as well (trace 1b). The same experiments were also carried out on a 5 s time scale (the kinetic traces of the transient species observed on a 5 s time scale, in reductions of NarGHI and NarI(ΔGH), were published by us previously (*1*)). All the kinetic features of the transient species observed on a 5 s time scale, for the wild-type enzyme and the mutants, were clearly exhibited on the longer time scale, 20 s, as shown in Figure 5. It was

Table 2: Kinetic Constants of Heme Reduction Observed on a 100 s Time Scale after Mixing 1 mg ML^{-1} $NarGHI^{H56R}$ or $NarGHI^{H205Y}$ with 500 μM Menadiol, Respectively, in the Absence and Presence of 60 μM HOQNO or STIG in 100 MM MOPS and 5 MM EDTA (pH7.0) at 25 °C

	heme reduction			heme reduction	
sample	k_1 (s^{-1})	k_2 (s^{-1})	sample	k_1 (s^{-1})	k_2 (s^{-1})
$NarGHI^{H56R}$	0.78 ± 0.08	0.03 ± 0.003	$NarGHI^{H205Y}$	0.04 ± 0.004	0.002 ± 0.0002
$NarGHI^{H56R}$/HOQNO	0.28 ± 0.03	0.016 ± 0.002	$NarGHI^{H205Y}$/HOQNO	0.034 ± 0.003	0.014 ± 0.001
$NarGHI^{H56R}$/STIG	0.19 ± 0.02	0.034 ± 0.003	$NarGHI^{H205Y}$/STIG	0.035 ± 0.004	0.004 ± 0.0004

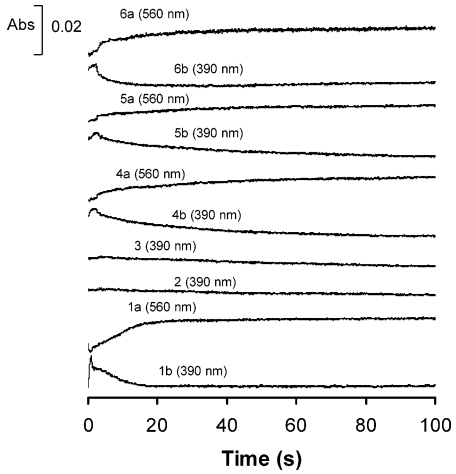

FIGURE 6: Observation of a transient species generated during the heme reduction by menadiol on a 100 s time scale. The absorbance traces were observed by rapidly mixing 1 mg mL^{-1} wild-type NarGHI and the mutants with 500 μM menadiol in 100 mM MOPS and 5 mM EDTA (pH 7.0) at 25 °C. Heme reductions were followed at 560 nm, and the corresponding traces were labeled with "a". The formations and decays of the transient species were monitored at 390 nm, and the traces were labeled with "b". Key: traces 1a and 1b, absorbance traces of heme reduction and the transient species for the wild-type NarGHI; traces 2 and 3, absorbance traces observed at 390 nm for $NarGHI^{H66Y}$ and $NarGHI^{H187Y}$, respectively; traces 4a and 4b, for $NarGHI^{H56R}$; traces 5a and 5b, for $NarGHI^{H205Y}$; traces 6a and 6b, for NarI(ΔGH). These traces were not shown with a common reference point of absorbance to avoid overlaps of them.

proposed by us recently that this transient species is a complex of semimenaquinone radical anion with the partially reduced enzyme (*1*).

Mutations of the heme-binding residues had significant effects on the formation of the transient species (Figure 5). For $NarGHI^{H66Y}$ (trace 2) and $NarGHI^{H187Y}$ (trace 3), lacking heme b_L and having heme b_H, the formation of the transient species was not observed nor was heme reduction (Figures 1 and 2). For $NarGHI^{H56R}$ (trace 4a) and $NarGHI^{H205Y}$ (trace 5a), without heme b_H but having heme b_L, the formation and decay of the transient species and heme reduction were observed (traces 4b and 5b). The decay of the transient species appeared to correlate to the relatively fast reduction phase of the heme. For NarI(ΔGH), which has no catalytic dimer NarGH, the formation and decay of the transient species were also observed (trace 6b), indicating that the decay of this species was not due to electron transfer from heme b_H to the catalytic dimer NarGH. The decay of the transient species, in fact, was correlated to the heme reduction (trace 6b) as observed for $NarGHI^{H56R}$ and $NarGHI^{H205Y}$.

To investigate the reaction processes described in Figure 5 on a longer time scale, the same experiments were repeated on a 100 s time scale. As shown in Figure 6, for the wild-type enzyme the decay of the transient species (trace 1a) was correlated to the heme reduction (trace 1b) and completed about 20 s after the mixing. The reduction of the hemes appeared to be saturated also within the same time scale as the decay of the transient species, about 20 s after the mixing. For mutants $NarGHI^{H66Y}$ (trace 2) and $NarGHI^{H187Y}$ (trace 3), there was no detectable formation of the transient species. For mutants $NarGHI^{H56R}$ (traces 4a an 4b), $NarGHI^{H205Y}$ (traces 5a and 5b), and NarI(ΔGH) (traces 6a and 6b), the formation and decay of the transient species as described in Figure 5 were observed and correlated to the heme reduction.

Reoxidation of Menadiol-Reduced Hemes in $NarGHI^{H56R}$ and $NarGHI^{H205Y}$ by Nitrate. To further investigate the role of the two hemes in the electron-transfer pathway from NarI to the catalytic dimer NarGH in NarGHI, a sequential stopped-flow method was adopted. In these experiments, 1 mg mL^{-1} membranes were mixed rapidly with 500 μM menadiol in 100 mM MOPS and 5 mM EDTA (pH 7.0) at 25 °C, which resulted in the heme reduction in the enzyme. After being aged for 50 s to allow complete heme reduction, this mixture was then rapidly mixed with 1 mM potassium nitrate solution in the same buffer. Using this method, the reoxidation of menadiol-reduced heme by nitrate was followed at 560 nm spectrophotometrically. As a control, the same sequential stopped-flow experiment was also carried out with LCB2048 membranes lacking NarGHI. For LCB2048 membranes, there was no significant absorbance change after rapid mixing with the nitrate solution, indicating that there was no reoxidation in the system (data not shown).

For NarGHI, as shown in Figure 7 (trace 1), a decrease of absorbance lasting for about 100 s was observed, indicating a reoxidation of the hemes. The data were fitted to eq 1, giving the rate constants k_1 of 0.19 ± 0.02 s^{-1} and k_2 of 0.01 ± 0.001 s^{-1}. For $NarGHI^{H66Y}$ (trace 2) and $NarGHI^{H187Y}$ (trace 3), lacking heme b_L and having heme b_H, there was no heme reoxidation since there was no heme reduction in the first place after the mutants were mixed with the menadiol solution (Figures 1 and 2). Interestingly, for $NarGHI^{H56R}$ (trace 4) or $NarGHI^{H205Y}$ (trace 5), without heme b_H but having heme b_L, significant heme reoxidation was not observed either, indicating that a single mutation of NarI-H56R or NarI-H205Y blocked the electron-transfer pathway from subunit NarI to the catalytic dimer NarGH by removing heme b_H.

When a lower concentration of menadiol (5 μM after 1:1 mixing) was used to reduce the wild-type enzyme and the mutants, the absorbance traces observed at 560 nm were very similar to those shown in Figure 7; i.e., a decrease of the absorbance at 560 nm was observed for the wild type and no significant absorbance change for all four mutants (data not shown).

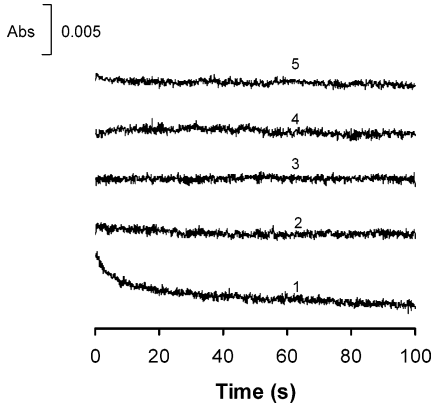

FIGURE 7: Reoxidation of menadiol-reduced hemes in the wild-type NarGHI and in the mutants by nitrate. The absorbance changes were observed at 560 nm, using a sequential stopped-flow method, after rapid mixing of 1 mg mL^{-1} NarGHI (trace 1), NarGHI^{H66Y} (trace 2), NarGHI^{H187Y} (trace 3), NarGHI^{H56R} (trace 4), and NarGHI^{H205Y} (trace 5) with 500 μM menadiol in 100 mM MOPS and 5 mM EDTA (pH 7.0) at 25 °C, and then mixing of the mixture with 1 mM nitrate in the same buffer. The fits to eq 1 gave the rate constants $k_1 = 0.19 \pm 0.02$ s^{-1} and $k_2 = 0.01 \pm 0.001$ s^{-1}, the amplitudes $A_1 = 0.0024$ and $A_2 = 0.0023$, and the residual of the fit of less than ± 0.00065 (not shown). These traces were not shown with a common reference point of absorbance to avoid overlaps of them.

DISCUSSION

In this study, we observed that, in NarGHI^{H66Y} and NarGHI^{H187Y}, lacking heme b_L but having b_H, heme reduction was abolished, whereas, in NarGHI^{H56R} and NarGHI^{H205Y}, a slower and smaller reduction appeared (Figures 1 and 2). These results indicate that electrons from menadiol are initially transferred to heme b_L, which is consistent with conventional spectrophotometric studies of mutants NarGHI^{H66Y} and NarGHI^{H56R} (*16*). This implies that it is easier for menadiol to access heme b_L and/or the binding site of menadiol is closer to heme b_L. Furthermore, the stopped-flow technique enables us to observe some kinetic features of heme reduction which cannot be observed using a conventional spectrophotometric method, for instance, the lag phases of heme reduction in NarGHI^{H56R} and NarGHI^{H205Y}.

A possible explanation for the lag phases is that these mutations may cause some conformational changes in the enzyme which alter the binding of menadiol. In other words, to bind menadiol, the mutant enzyme may have to first make some conformational adjustments to restore the regional conformational structures disturbed by the mutation, which could lead to the appearance of a lag phase. During the time period of this lag phase, a very slow heme reduction may occur by transfer of the first electron from bound menadiol. Following the lag phase, the relatively fast reduction of heme observed could be due to receipt of the second electron from the menadione radical anion (see below). These mutations not only caused a lag phase for the heme reduction but also reduced the rate of the reduction significantly as shown in Table 1.

The magnitude of heme reduction in NarGHI^{H56R} was larger than that in NarGHI^{H205Y} (Figure 2). It is likely that the mutations NarGHI^{H56R} and NarGHI^{H205Y} may not only eliminate heme b_H binding but also result in changes in the environment of heme b_L. These changes could lead to an enhancement of heme reduction in the case of NarGHI^{H56R} (but still smaller than in the wild-type enzyme) or a decrease of heme reduction in NarGHI^{H205Y}.

Heme reduction by menadiol was not observed in mutants NarGHI^{H66Y} and NarGHI^{H187Y} lacking heme b_L. However, when dithionite was used as a reducing agent, heme reduction was observed in both mutants (data not shown). These findings indicate that heme reduction by dithionite proceeds with a mechanism different from that of heme reduction by menadiol. It seems likely that menadiol can only access heme b_L or the menadiol binding site may be closer to heme b_L, and thus, electrons from menadiol could only be delivered to heme b_L. Dithionite molecules, on the other hand, may be able to access not only heme b_L but also heme b_H and to reduce them easily when whichever is available.

The effects of quinol-binding-site inhibitors HOQNO and STIG on heme reduction in NarGHI^{H56R} and NarGHI^{H205Y} appeared to be different. For NarGHI^{H56R} (Figure 3), HOQNO exhibited a less inhibitory effect than STIG on heme reduction. For NarGHI^{H205Y} (Figure 4), however, both inhibitors showed a similar level of inhibition of heme reduction. These different inhibitory effects for different mutants are also demonstrated in the rate constants as shown in Table 2. We have reported the inhibition of HOQNO and STIG on heme reduction by menadiol in the wild-type NarGHI (*1*). The binding of HOQNO to the wild-type enzyme caused a dramatic change of the kinetic pattern of heme reduction; the four-phase kinetic pattern (as described for Figures 1 and 2) was replaced by a clear-cut two-phase kinetic profile, and the reoxidation phase (phase 2 of heme reduction for the wild type) disappeared (*1*). The loss of the reoxidation phase by HOQNO binding to the wild-type enzyme implies that HOQNO is still bound to the enzyme during the reduction processes induced by menadiol binding. Since both HOQNO and menadiol are menaquinol analogues, we suggested that there may be more than one menaquinol binding site (Q-site) in the wild-type enzyme.

For NarGHI^{H56R} (Figure 3) and NarGHI^{H205Y} (Figure 4), the change of the kinetic pattern of heme reduction caused by HOQNO binding was not as dramatic as for the wild-type enzyme. In fact, except for the loss of the relatively fast reduction phase, the kinetic pattern overall was quite similar to that observed in the absence of HOQNO. It can thus be speculated that mutants NarGHI^{H56R} and NarGHI^{H205H} not only eliminate heme b_H but may also disturb or even eliminate the alternative MQH_2 binding site specifically for HOQNO. This speculation is in line with the suggestions that the location of this site may be close to heme b_H (*18*). In other words, in NarGHI^{H56R} and NarGHI^{H205Y}, there may be only one MQH_2 binding site left and the reduction of the enzyme preincubated with HOQNO can only take place after a ligand exchange of replacing HOQNO by menadiol in the binding site. After binding of menadiol to the enzyme, the heme reduction would proceed with the kinetic pattern similar to that in the absence of HOQNO.

The transient species observed at 390 nm in the wild-type NarGHI has been assigned to a menadione radical anion ($MQ^{\bullet -}$) associated with the enzyme (*1*). The free menadione radical anion has an absorption maximum at 390 nm (*30*, *31*) with a molar extinction coefficient of 13000 M^{-1} cm^{-1} (*30*). The molar extinction coefficient of the transient species observed at 390 nm during heme reduction in the wild-type enzyme has been calculated to be about 14000 M^{-1} cm^{-1}

(*1*). For NarGHI^{H56R}, NarGHI^{H205Y}, and NarI(ΔGH), the transient species observed at 390 nm has a molar extinction coefficient of approximately 12000 M^{-1} cm^{-1}, calculated using the absorbance value (about 0.012) and the concentration of the mutant proteins (1 μM after 1:1 mixing with menadiol solution). The transient species observed at 390 nm during menadiol-induced heme reduction in NarGHI^{H56R}, NarGHI^{H205Y}, and NarI(ΔGH) would be similar to the one observed in the wild-type NarGHI, a menadione radical anion but associated with the mutants in this case.

The formation of this semimemaquinone species ($MQ^{\bullet-}$ enzyme) during menadiol-induced heme reduction in the mutants is the result of menadiol oxidation followed by deprotonation, losing two protons, as we proposed for the wild-type enzyme (*1*). The observation of the formation and decay of the transient species in NarI(ΔGH) indicates its formation and decay are not related to the catalytic dimer NarGH since there is no NarGH in NarI(ΔGH). As shown in Figures 5 and 6, the decay of this transient species is correlated with heme reduction. However, this transient species is not formed as the result of heme reduction, because it is not observed in heme reduction by dithionite. This conclusion agrees with the mechanism proposed by us recently that this transient species is formed from menadiol (a semimemaquinone radical anion) and its decay would be due to the electron transfer from it to heme b_L in the enzyme (*1*).

After rapid mixing of menadiol-reduced NarGHI or the mutants with nitrate (Figure 7), nitrate binds to the reduced enzyme to form a complex of nitrate and the enzyme. Upon the formation of the complex, the reduced enzyme delivers two electrons to nitrate to yield nitrite, and takes two protons from the cytoplasmic side of the membrane. This is followed by release of the nitrite and a water molecule from the complex. The reduction of nitrate by the reduced enzyme would induce the oxidation of the Mo-bisMGD cofactor that would in turn withdraw an electron from the reduced iron−sulfur clusters. This would initiate a series of electron-transfer processes, from the reduced hemes to the reoxidized iron−sulfur cluster, resulting in the reoxidation of the hemes, and from the reduced iron−sulfur clusters to the oxidized Mo-bisMGD cofactor (*1*).

One may ask, after heme reduction in NarGHI^{H56R} and NarGHI^{H205Y} (Figures 1 and 2), whether electrons received by heme b_L from menadiol can be transferred directly to the catalytic dimer NarGH in the absence of heme b_H. As shown in Figure 7, for menadiol-reduced NarGHI^{H56R} or NarGHI^{H205Y} (in which the heme b_L was reduced), the reoxidation of the reduced heme by nitrate did not occur. This clearly indicates that heme b_H is a necessary component in the electron-transfer pathway and without heme b_H electrons cannot be transferred from heme b_L to the catalytic dimer NarGH.

In summary, this is the first report of a stopped-flow study of heme reduction by menadiol and heme reoxidation by nitrate in NarGHI^{H56R}, NarGHI^{H205Y}, NarGHI^{H66Y}, and NarGHI^{H187Y}. The results indicate that without heme b_L electrons cannot be transferred from MQH_2 to heme b_H. On the other hand, in the absence of heme b_H, electrons cannot be transferred from the reduced heme b_L to the catalytic dimer NarGH. Therefore, both hemes are crucial components in the electron-transfer pathway from the subunit NarI through subunit NarH to the catalytic subunit NarG. A transient species, described as a complex of menadione radical anion associated with the enzyme, is formed during the process of heme reduction by menadiol.

ACKNOWLEDGMENT

We thank Dr. F. Blasco of the Laboratoire de Chimie Bacterienne, IBSM, CNRS, Marseille, France, for supplying the nitrate reductase plasmids, Dr. C. Kay of the Department of Biochemistry, University of Alberta, for providing the stopped-flow facility, and Ms. D. Mroczko of the Department of Biochemistry, University of Alberta, for preparing the cells.

REFERENCES

1. Zhao, Z., Rothery, R. A., and Weiner, J. H. (2003) *Biochemistry 42*, 5403−5413.
2. Gennis, R. B., and Ferguson-Miller, S. (1996) *Curr. Biol. 6*, 36−8.
3. Rothery, R. A., Magalon, A., Giordano, G., Guigliarelli, B., Blasco, F., and Weiner, J. H. (1998) *J. Biol. Chem. 273*, 7462−7469.
4. Magalon, A., Asso, M., Guigliarelli, B., Rothery, R. A., Bertrand, P., Giordano, G., and Blasco, F. (1998) *Biochemistry 37*, 7363−7370.
5. Augier, V., Asso, M., Guigliarelli, B., More, C., Bertrand, P., Santini, C. L., Blasco, F., Chippaux, M., and Giordano, G. (1993) *Biochemistry 32*, 5099−5108.
6. Guigliarelli, B., Magalon, A., Asso, M., Bertrand, P., Frixon, C., Giordano, G., and Blasco, F. (1996) *Biochemistry 35*, 4828−4836.
7. Hacket, N. R., and Bragg, P. D. (1982) *FEMS Microbiol. Lett. 13*, 213-217.
8. Magalon, A., Rothery, R. A., Giordano, G., Blasco, F., and Weiner, J. H. (1997) *J. Bacteriol. 179*, 5037−45.
9. Rothery, R. A., Blasco, F., Magalon, A., Asso, M., and Weiner, J. H. (1999) *Biochemistry 38*, 12747−12757.
10. Jones, R. W., Lamont, A., and Garland, P. B. (1980) *Biochem. J. 190*, 79−94.
11. Blasco, F., Iobbi, C., Giordano, G., Chippaux, M., and Bonnefoy, V. (1989) *Mol. Gen. Genet. 218*, 249−256.
12. Richardson, D. J., and Watmough, N. J. (1999) *Curr. Opin. Chem. Biol. 3*, 207−219.
13. Jormakka, M., Tornroth, S., Byrne, B., and Iwata, S. (2002) *Science 295*, 1863−8.
14. Blasco, F., Guigliarelli, B., Magalon, A., Asso, M., Giordano, G., and Rothery, R. A. (2001) *Cell. Mol. Life Sci. 58*, 179−193.
15. Rothery, R. A., Blasco, F., Magalon, A., and Weiner, J. H. (2001) *J. Mol. Microbiol. Biotechnol. 3*, 273−283.
16. Magalon, A., Rothery, R. A., Lemesle-Meunier, D., Frixon, C., Weiner, J. H., and Blasco, F. (1998) *J. Biol. Chem. 273*, 10851−10856.
17. Morpeth, F. F., and Boxer, D. H. (1985) *Biochemistry 24*, 40−46.
18. Giordani, R., Buc, J., Cornish-Bowden, A., and Cardenas, M. L. (1997) *Eur. J. Biochem. 250*, 567−577.
19. Rothery, R. A., Blasco, F., and Weiner, J. H. (2001) *Biochemistry 40*, 5260−5268.
20. Magalon, A., Lemesle-Meunier, D., Rothery, R. A., Frixon, C., Weiner, J. H., and Blasco, F. (1997) *J. Biol. Chem. 272*, 25652−25658.
21. Zhao, Z., and Weiner, J. H. (1998) *J. Biol. Chem. 273*, 20758−20763.
22. Zhao, Z., Rothery, R. A., and Weiner, J. H. (1999) *Eur. J. Biochem. 260*, 50−56.
23. Hagerhall, C., Magnitsky, S., Sled, V. D., Schroder, I., Gunsalus, R. P., Cecchini, G., and Ohnishi, T. (1999) *J. Biol. Chem. 274*, 26157−64.
24. Hastings, S. F., Kaysser, T. M., Jiang, F., Salerno, J. C., Gennis, R. B., and Ingledew, W. J. (1998) *Eur. J. Biochem. 255*, 317−23.
25. Veselov, A. V., Osborne, J. P., Gennis, R. B., and Scholes, C. P. (2000) *Biochemistry 39*, 3169−75.
26. Blasco, F., Nunzi, F., Pommier, J., Brasseur, R., Chippaux, M., and Giordano, G. (1992) *Mol. Microbiol. 6*, 209−219.

27. Rothery, R. A., and Weiner, J. H. (1991) *Biochemistry 30*, 8296−8305.
28. Markwell, M. A. D., Haas, S. M., Bieber, L. L., and Tolbert, N. E. (1978) *Anal. Biochem. 87*, 206−210.
29. Rothery, R. A., Chatterjee, I., Kiema, G., McDermott, M. T., and Weiner, J. H. (1998) *Biochem. J. 332* (Part 1), 35−41.
30. Rao, P. S., and Hayon, E. (1973) *J. Phys. Chem. 77*, 22742276.
31. Patel, K. B., and Willson, R. L. (1973) *J. Chem. Soc., Faraday Trans. 1 69*, 814−825.

BI0350856